Journal of Solid State Chemistry 183 (2010) 120–127

Contents lists available at ScienceDirect

Journal of Solid State Chemistry

journal homepage: www.elsevier.com/locate/jssc

MAS-NMR studies of lithium aluminum silicate (LAS) glasses and glass–ceramics having different Li_2O/Al_2O_3 ratio

A. Ananthanarayanan [a], G.P. Kothiyal [a,*], L. Montagne [b], B. Revel [b]

[a] Technical Physics and Prototype Engineering Division, Bhabha Atomic Research Centre, Mumbai 400085, India
[b] UCCS - Unité de Catalyse et Chimie du Solide – UMR CNRS 8181, Ecole Nationale Supérieure de Chimie de Lille, Université des Sciences et Technologies de Lille, BP 108, 59562 Villeneuve d' Ascq Cedex, France

ARTICLE INFO

Article history:
Received 31 July 2009
Received in revised form
14 October 2009
Accepted 15 October 2009
Available online 3 November 2009

Keywords:
Glass
Glass–ceramics
Silicates
Crystallization
MAS-NMR
XRD

ABSTRACT

Emergence of phases in lithium aluminum silicate (LAS) glasses of composition (wt%) xLi_2O–$71.7SiO_2$–$(17.7-x)Al_2O_3$–$4.9K_2O$–$3.2B_2O_3$–$2.5P_2O_5$ ($5.1 \le x \le 12.6$) upon heat treatment were studied. ^{29}Si, ^{27}Al, ^{31}P and ^{11}B MAS-NMR were employed for structural characterization of both LAS glasses and glass–ceramics. In glass samples, Al is found in tetrahedral coordination, while P exists mainly in the form of orthophosphate units. B exists as BO_3 and BO_4 units. ^{27}Al NMR spectra show no change with crystallization, ruling out the presence of any Al containing phase. Contrary to X-ray diffraction studies carried out, ^{11}B (high field 18.8 T) and ^{29}Si NMR spectra clearly indicate the unexpected crystallization of a borosilicate phase $(Li,K)BSi_2O_6$, whose structure is similar to the aluminosilicate virgilite. Also, lithium disilicate ($Li_2Si_2O_5$), lithium metasilicate (Li_2SiO_3) and quartz (SiO_2) were identified in the ^{29}Si NMR spectra of the glass–ceramics. ^{31}P NMR spectra of the glass–ceramics revealed the presence of Li_3PO_4 and a mixed phase $(Li,K)_3PO_4$ at low alkali concentrations.

1. Introduction

Lithium aluminum silicate (LAS) glass–ceramics combine a wide variety of useful properties such as good mechanical strength, resistance to thermal shock, high chemical durability and creep resistance [1–5]. As a result these glass–ceramics see extensive applications in heat exchangers, cookware, telescope mirror supports, etc. [6,7]. In particular, LAS glass–ceramics derived from the Li_2O–K_2O–Al_2O_3–SiO_2–B_2O_3–P_2O_5 system, with lithium disilicate as the major crystalline phase, are used in hermetic sealing to metals with high thermal expansion coefficients (TECs) [8–10]. Similar glass–ceramics are also being evaluated as prospective dental materials [11,12]. Previously we have investigated phase emergence in this system as a function of composition and the attendant effect on thermo-physical properties [13]. Phase identification was achieved by X-ray diffraction (XRD). We have observed that at low Al_2O_3 contents, lithium disilicate was the major phase formed, while at higher Al_2O_3 content, either quartz or a stuffed derivative (eucryptite) was crystallized. The close proximity of quartz and stuffed quartz XRD peaks made unambiguous phase assignment difficult [14].

MAS-NMR enables an accurate identification of structural units, especially in glasses, and simultaneously achieves phase identification complementary to XRD in glass ceramics. Binary compositions of the type M_2O–SiO_2 (where M=Li, Na) have been extensively investigated by MAS-NMR techniques. These compositions were studied either to understand the validity of structural models or to comprehend the change in speciation (Q^n) during crystallization of these glasses [15–19]. While the binary lithium disilicate system has been the focus of numerous NMR investigations, to the best of our knowledge, no work studying the Li_2O–K_2O–Al_2O_3–SiO_2–B_2O_3–P_2O_5 system using MAS-NMR is available.

Therefore, we have studied the effect of composition and crystallization on glasses/glass–ceramics having general composition (wt%) xLi_2O–$71.7SiO_2$–$(17.7-x)Al_2O_3$–$4.9K_2O$–$3.2B_2O_3$–$2.5P_2O_5$ ($5.1 \le x \le 12.6$) by means of ^{29}Si, ^{27}Al, ^{31}P and ^{11}B magic angle spinning nuclear magnetic resonance (MAS-NMR) spectroscopy. The motivation for MAS-NMR studies as a function of the Li_2O/Al_2O_3 ratio is to investigate the local environments of Si, B, Al and P in both glass and glass–ceramic samples and correlate the phase emergence in these LAS glasses upon controlled heat treatment. The Li chemical shifts are not resolved for Li_3PO_4, $Li_2Si_2O_5$ or Li^+ in the residual glass [15]; hence $^{6,7}Li$ NMR was not used in the present study.

2. Experimental

The compositions of the glasses are listed in Table 1, along with the assigned nomenclature (L1 to L5). The glasses were

* Corresponding author.
E-mail address: gpkoth@barc.gov.in (G.P. Kothiyal).

0022-4596/$ - see front matter © 2009 Elsevier Inc. All rights reserved.
doi:10.1016/j.jssc.2009.10.006

Table 1
Compositions of LAS glasses.

Composition	L1		L2		L3		L4		L5	
	mol%	wt%	mol%	wt%	mol%	wt%	mol%	wt%	mol%	wt%
SiO_2	67.0	71.7	68.9	71.7	71.7	71.7	72.3	71.7	74.4	71.7
Li_2O	23.7	12.6	20.5	10.6	17.3	8.8	14.4	7.1	10.7	5.1
Al_2O_3	2.8	5.1	4.0	7.1	4.8	8.9	6.3	10.6	7.7	12.6
K_2O	2.9	4.9	3.0	4.9	3.1	4.9	3.2	4.9	3.2	4.9
B_2O_3	2.6	3.2	2.7	3.2	2.7	3.2	2.8	3.2	2.9	3.2
P_2O_5	1.0	2.5	1.0	2.5	1.1	2.5	1.1	2.5	1.1	2.5

Batch compositions.

prepared using the melt quench technique. Analytical grade precursors (Li_2CO_3, Al_2O_3, SiO_2, B_2O_3, $NH_4H_2PO_4$ and KNO_3) were mixed thoroughly and calcined in alumina crucibles according to a schedule determined by the decomposition temperatures of the precursors. To ensure complete decomposition of nitrates and carbonates into oxides, the batch was weighed before and after calcination to ascertain weight loss. The calcined batch was melted under ambient air at 1500–1550 °C in a Pt–Rh crucible in a raising lowering hearth electric furnace (Model OKAY M/s Bysakh and Co. Kolkata) and held for 1–2 h to ensure melt homogenization. The melt was poured onto pre-heated graphite molds and annealed at 500–550 °C for 3–4 h to relieve thermal stresses. Glass samples were crystallized according to the schedule given in Table 2. The thermo-physical and structural features of the LAS glasses and glass ceramics were reported by us previously [13].

^{29}Si, ^{27}Al, ^{11}B and ^{31}P MAS-NMR spectra were recorded at 2.34, 18.8, 18.8 and 9.4 T, respectively, on Bruker AVANCE spectrometers, with 4 mm probes at 12.5 kHz spinning speed, excepted for ^{29}Si for which a 7 mm probe at 8 kHz was used. The Larmor frequencies were 19.8, 208.5, 256.8 and 128.3 MHz for ^{29}Si, ^{27}Al, ^{11}B and ^{31}P, respectively. For ^{31}P, the pulse duration was 1.6 μs ($\pi/6$), and the recycle delay was 120 s. For ^{11}B, the pulse duration was 2 μs ($\pi/6$), and the recycle delay was 10 s. For ^{27}Al, the pulse duration was 1.5 μs ($\pi/8$), and the recycle delay was 2 s. For ^{29}Si, the pulse duration was 1.6 μs ($\pi/5$), and the recycle delay was 180 s. All relaxation delays were chosen long enough to enable relaxation at the field strength that was used. The ^{29}Si chemical shifts are relative to tetramethyl silane (TMS) at 0 ppm, those of ^{27}Al is relative $Al(H_2O_6)^{3+}$ species at 0 ppm in 1M $Al(NO_3)_3$ solution, those of ^{11}B nuclei are given relative to BPO_4 at 3.6 ppm and those of ^{31}P is relative to 85% H_3PO_4 at 0 ppm. The decomposition of NMR spectra was carried out using DM-FIT software [20]. We fitted ^{29}Si and ^{31}P NMR spectra of glasses using a Gaussian lineshape, while a Lorentzian lineshape was found more suitable for the crystalline phases.

Table 2
Crystallization schedule for LAS glass samples.

Sample name	T_1 (°C)	Dwell time at T_1 (h)	T_2 (°C)	Dwell time at T_2 (h)
L-1	600	2	800	3
L-2	600	2	800	3
L-3	600	2	640	3
L-4	600	2	925	3
L-5	700	2	740	3

T_1 and T_2 are the first and second holding temperatures for crystallization.

Table 3
Thermo-physical properties of lithium aluminum silicate glasses/glass–ceramics (L-1 to L-5).

Sample name	TEC ($\times 10^{-6}$/°C) (±5%)	T_g (°C) (±5 °C)	MH (GPa)	Density (g/cc)
L-1 Glass	10.5	543	5.73(2)	2.40(1)
L-1GC	9.5	584	7.66(3)	2.40(2)
L-2 Glass	8.6	485	5.86(5)	2.43(1)
L-2 GC	9.6	–	7.45(4)	2.44(2)
L-3 Glass	8.3	483	5.92(6)	2.45(2)
L-3 GC	9.8	567	8.45(2)	2.46(3)
L-4 Glass	7.8	587	6.04(3)	2.47(1)
L-4 GC	5.3	597	7.38(5)	2.47(2)
L-5 Glass	7.6	432	6.13(3)	2.50(3)
L-5 GC	4.5	568	6.68(3)	2.54(2)

The error in microhardness (MH) and density is the observed standard deviations for atleast 10 measurements.

3. Results

3.1. Thermo-physical properties and XRD

The thermo-physical properties of the LAS glasses and glass ceramics are listed in Table 3. With the increase of Al_2O_3 at the expense of Li_2O in L1 to L5 glasses, microhardness (MH) shows a monotonous increase, while TEC reduces. Such a compositional dependence breaks down in case of glass–ceramics, influenced by the formation of various crystalline phases. The X-rays diffractograms of the glass–ceramics are shown in Fig. 1. In L1 glass–ceramic, lithium disilicate ($Li_2Si_2O_5$) (pdf 00-040-0376) is the major crystalline phase and a small amount of quartz (SiO_2) (pdf 00-012-0708) is found. L2 glass–ceramic contains lithium disilicate and quartz, and a very small amount of a lithium aluminosilicate phase, called virgilite $Li_xAl_xSi_{(3-x)}O_6$ (pdf 00-031-0707). This virgilite phase is actually a borosilicate phase, as will be shown below, hence it will be called "alumino-borosilicate phase" in the following text. Quartz and lithium metasilicate (pdf 00-029-0829) are the two crystalline phase detected in L3 glass ceramic. A small amount of lithium metasilicate is still detected in L4, while quartz and an alumino-borosilicate phase are the main phases. The alumino-borosilicate phase is the only crystalline phase present in L5 glass–ceramic.

X-rays diffractograms assignment of LAS glass–ceramics is not easy due to the low signal to noise ratio (a large amount of glass phase is still present as will be shown on NMR spectra), and the phase identification is not straightforward due to the presence of many light elements and of phases with close structural characteristics. For instance, it is difficult to discern quartz from its stuffed derivatives such as virgilite ($Li_xAl_xSi_{3-x}O_6$) phase using XRD [14]. This was a motivation for recording NMR spectra of the samples.

3.2. ^{29}Si MAS-NMR

The ^{29}Si MAS-NMR spectra of the LAS glasses are reported in Fig. 2. These show a broad feature in the −70 to −120 ppm range. This was assumed to be a convolution of three resonances at ~−103, −90 and −79 ppm. These resonances are attributed the Q^4, Q^3 and Q^2 structural units, respectively, as found in other aluminosilicate glasses [21–24]. In the ^{29}Si NMR spectra of the glasses, it is observed that L1 and L2 spectra are similar and the shape of the spectra changes between L2 and L3, with L4 and L5 being similar to L3. From L2 to L3 the broad resonance shifts to more negative values. It is likely that with a reduction in the modifier fraction, Q^4 sites become more prevalent. Further, the shifts of the resonances of L3 to L5 glasses to higher chemical shift values (i.e. less negative values) compared to pure silica are attributed to the presence of Si–O–Al bonds and to a lesser extent of Si–O–B bonds [25,26].

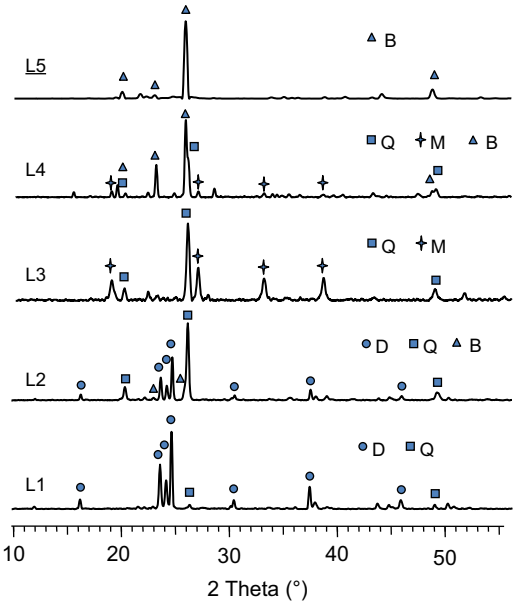

Fig. 1. X-ray diffractograms of lithium aluminum silicate (LAS) glass–ceramics (see Table 1 for the compositions), Q=SiO_2 (pdf 00-012-0708), D=$Li_2Si_2O_5$ (pdf 00-040-0376), M=$LiSiO_3$ (pdf 00-029-0829), B=$Li_xAl_xSi_{(3-x)}O_6$/(Li,K)BSi_2O_6 (pdf 00-031-0707).

The ^{29}Si NMR spectra for the LAS glass–ceramics are shown in Fig. 3. They contain sharp peaks superimposed on a broad resonance. The latter is characteristic of the residual glass. The narrow peak observed at −92 ppm on L1 glass–ceramic spectrum is assigned to lithium disilicate [27], in accordance with XRD (Fig. 1). We notice that no other resonance is observed on this spectrum, while XRD indicated the presence of a small amount of quartz phase. L2 glass–ceramic spectrum also shows the lithium disilicate resonance at −92 ppm, together with two resonances at −107 and −113 ppm. They can be assigned to quartz (SiO_2) and tridymite (SiO_2), respectively [28]. However, the observation of a tridymite resonance contradicts the X-ray diffractograms shown in Fig. 1. An alumino-borosilicate phase is indeed observed on the X-ray diffractogram of the L2 glass–ceramic. Nevertheless, this −113 ppm resonance is assigned to a boron-containing phase ((Li,K)BSi_2O_6), as will be justified later. We notice that this phase is clearly visible on the NMR spectrum while it is hardly visible on the X-ray diffractogram of L2. L3 glass–ceramic spectrum shows a small resonance at −75 ppm. This chemical shift is characteristic of a silicate phase with a low polymerization degree, i.e. lithium metasilicate [27], in accordance with XRD (Fig. 1). A small amount of quartz was also detected with XRD, which is visible on the NMR spectrum as a small feature on top of the broad glass resonance. L4 spectrum also shows the metasilicate resonance at −75 ppm, but with a low intensity as in XRD, and quartz and the alumino-borosilicate resonances are visible at −107 and −113 ppm. The L5 glass–ceramic spectrum shows the same resonances at −107 and −113 ppm, while the metasilicate resonance disappeared.

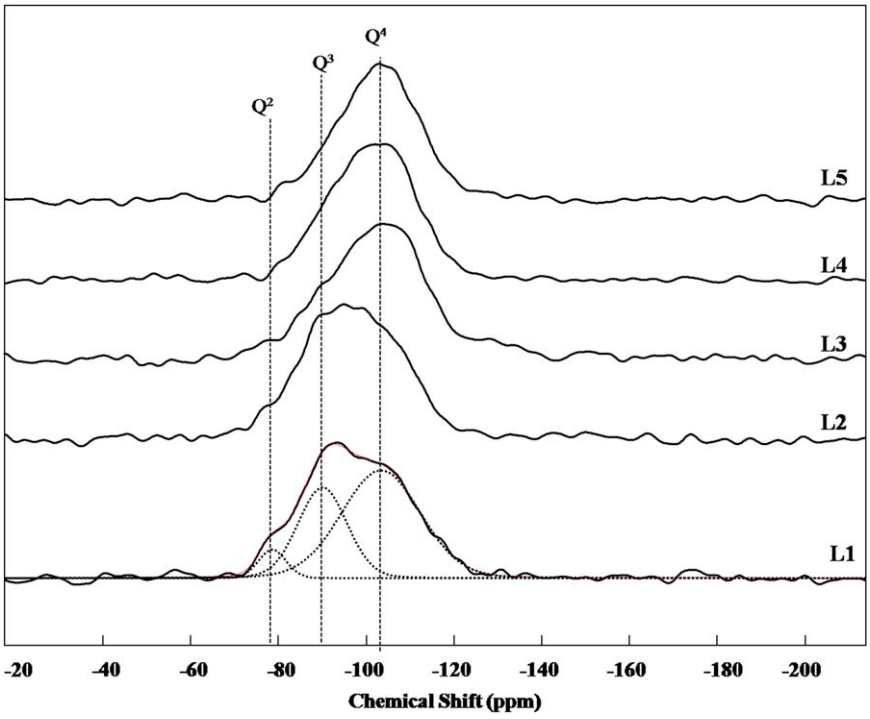

Fig. 2. ^{29}Si MAS-NMR spectra of LAS glasses. Typical spectrum decomposition is shown for L1 glass. The estimated positions of Q^2, Q^3 and Q^4 resonances are indicated.

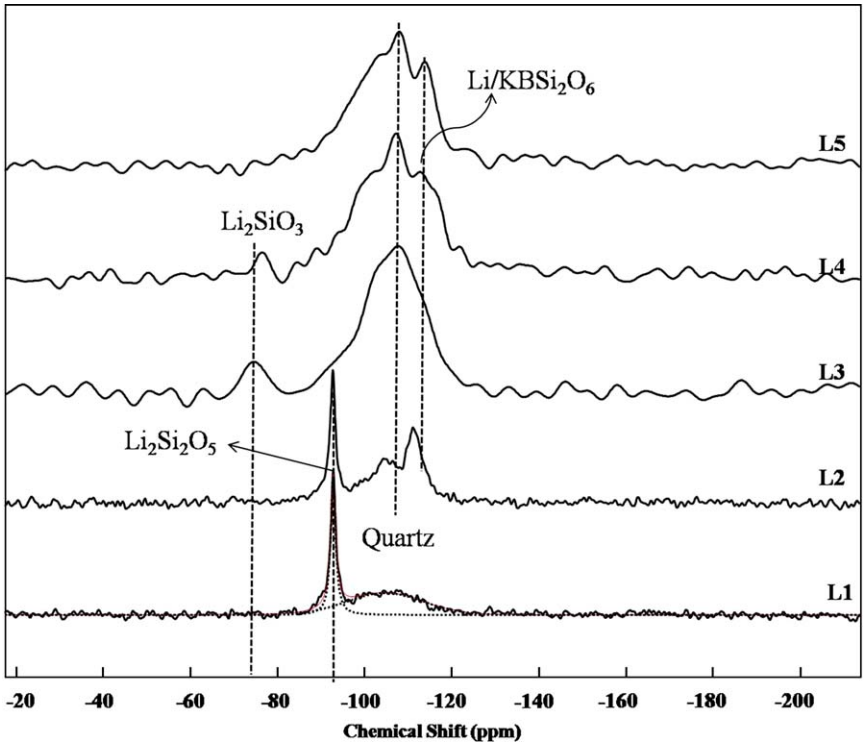

Fig. 3. ^{29}Si MAS-NMR spectra of LAS glass–ceramics.

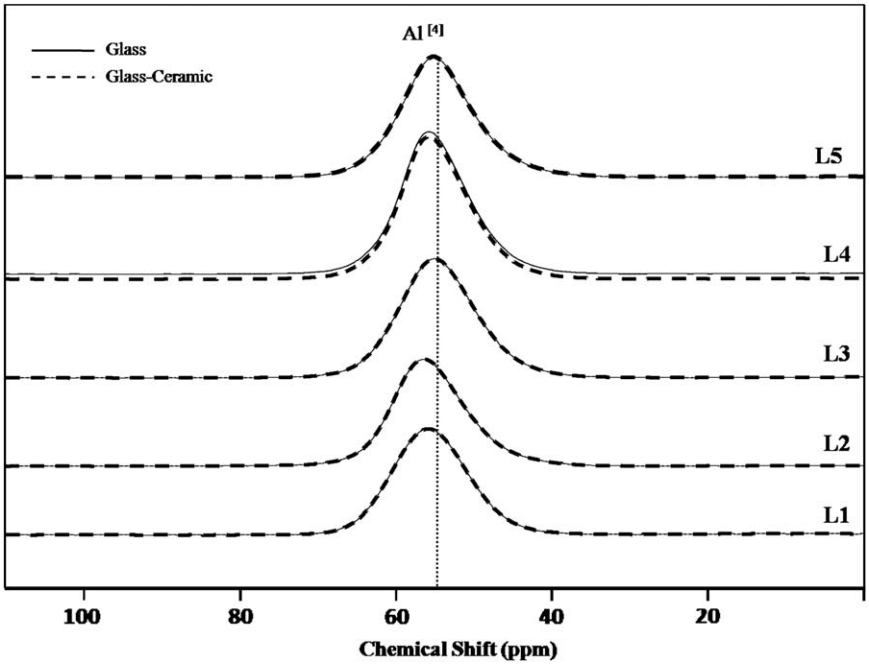

Fig. 4. ^{27}Al MAS-NMR spectra of LAS glasses, superimposed on those of respective LAS glass–ceramics (dashed lines).

On L4 and L5 glass–ceramic spectra, the presence of two resonances at −107 and −113 ppm may be questioned owing to their low intensity. In order to improve the spectrum quality, a large number (NS) of FIDs (free induction decays), NS=1360, was accumulated to improve signal to noise ratio. Then, a long relaxation delay (900 s, with NS=288) was used in order to check if signal intensity was affected by insufficient relaxation. Both experimental conditions did not change significantly the resulting spectrum, but they enabled to confirm the presence of the two narrow resonances at −107 and −113 ppm, in addition to the residual glass signal.

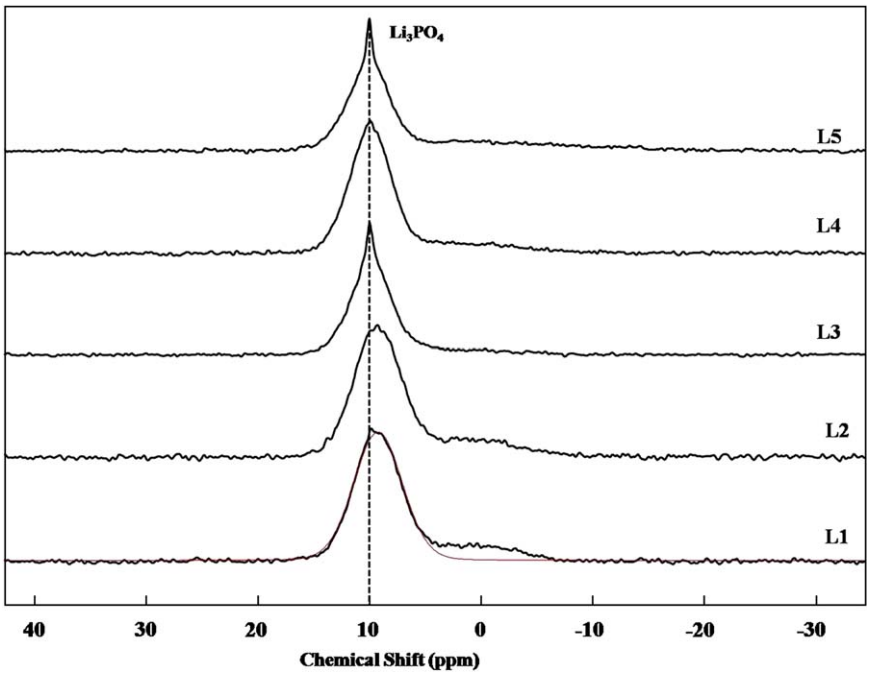

Fig. 5. ^{31}P MAS-NMR spectra of LAS glasses.

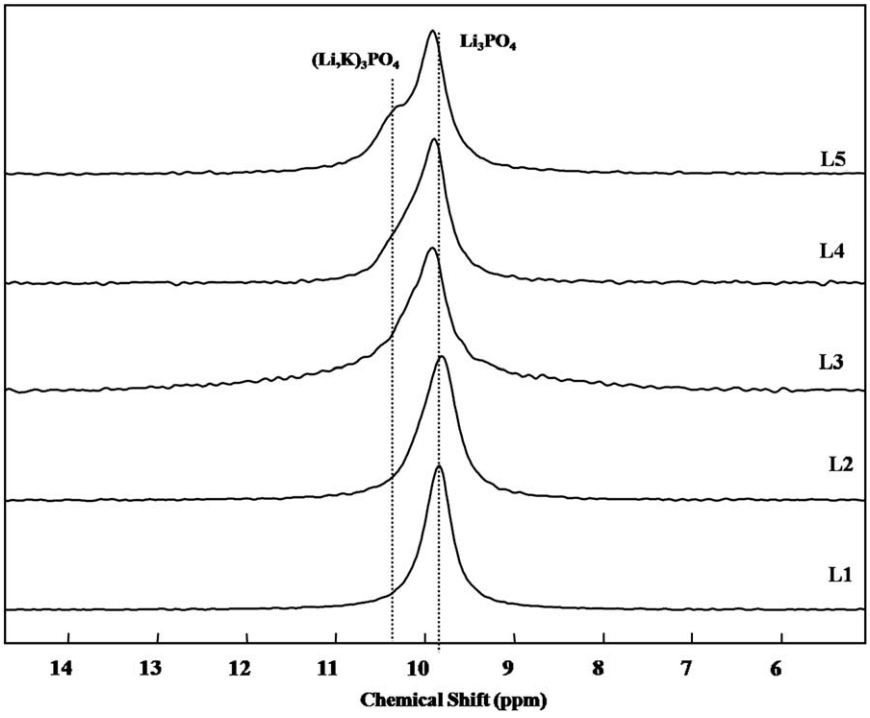

Fig. 6. ^{31}P MAS-NMR spectra of LAS glass–ceramics.

3.3. ^{27}Al MAS-NMR

The ^{27}Al NMR spectra for LAS glasses and glass–ceramics are reported in Fig. 4. The spectrum of each glass–ceramic is superimposed on the spectrum of the respective parent glass. It is observed that the ^{27}Al NMR spectra of each parent glasses and glass–ceramics are identical. The spectra consist of a broad resonance centered at ~55 ppm, which is characteristic of tetrahedral AlO_4 structural units [29].

3.4. ^{31}P MAS-NMR

The ^{31}P NMR spectra of the glasses are shown in Fig. 5. A main broad resonance is observed at 9 ppm, which is assigned to Q^0 (orthophosphate units) [30]. A second broad minor contribution at ~0 ppm can be assigned to Q^1 (pyrophosphate units) [30]. It is observed that some crystallization of Li_3PO_4 has occurred in L3 and L5 glasses, characterized by the presence of a narrow peak at 10 ppm. Since the P_2O_5 quantity is small in these glasses,

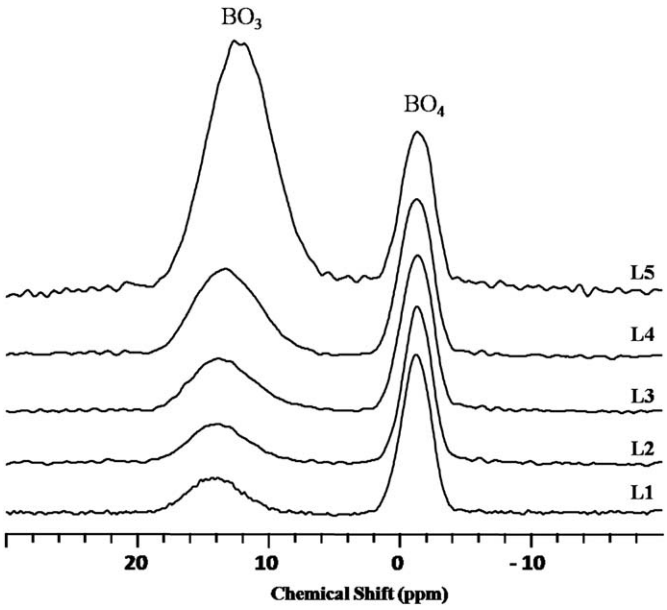

Fig. 7. ^{11}B MAS-NMR spectra of LAS glasses.

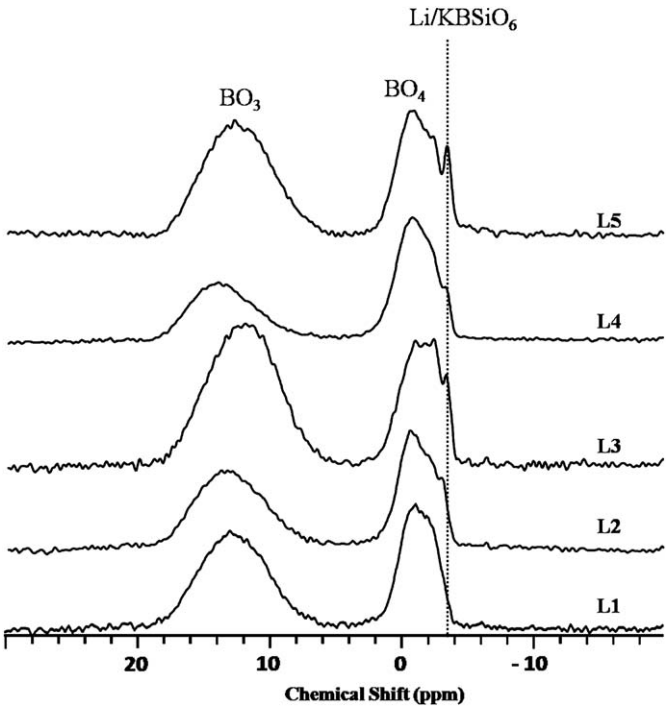

Fig. 8. ^{11}B MAS-NMR spectra of LAS glass–ceramics.

phosphate crystals were not detected by XRD analyses carried out on the parent glasses.

The ^{31}P NMR spectra of the LAS glass–ceramics are shown in Fig. 6. The reduction in the width of the resonances compared to the glass samples spectra (Fig. 5) implies that the P atoms are in a regular crystalline environment. The most evident feature is the peak at 9.8 ppm. This peak corresponds to Li_3PO_4 [16]. As the alkali oxide content decreases in L3 to L5 glass–ceramic spectra, we observe the presence of a shoulder centered on 10.5 ppm. This chemical shift does not correspond to that of K_3PO_4 (at 11.7 ppm [31]). It is known that ^{31}P chemical shift is sensitive to the average cationic field strength in the second coordination sphere of phosphorus [32], hence we suggest that the observed chemical shift can be attributed to the crystallization of mixed Li, K orthophosphate phase.

3.5. ^{11}B MAS-NMR

The ^{11}B NMR spectra of the parent glasses are shown in Fig. 7. The spectra consist of two resonances centered on -14 and -1 ppm. The use of a high-field spectrometer enables us to obtain well resolved resonances, almost free of second order quadrupolar broadening. The resonances can be assigned to BO_3 and BO_4 units, respectively [33]. It is observed that the relative fraction of BO_3 units increases when the alkali oxide fraction decreases in the glasses. This is due to the decrease in the quantity of cations available for the charge compensation of BO_4 groups.

An interesting feature is visible on the NMR spectra of the glass–ceramics shown in Fig. 8. A sharp resonance at -3.3 ppm appears on the BO_4 resonance that indicates the crystallization of a boron-containing phase. To our knowledge, the crystallization of a boron-containing phase in multicomponent LAS glass–ceramics has never been reported in the literature. It is likely that without the NMR analysis, this phase (containing light elements) would have been classified as an isostructural aluminosilicate phase with XRD. This point is considered in the discussion section.

4. Discussion

In LAS glass–ceramics, the thermo-physical properties are strongly dependent upon the nature and relative fractions of the various phases. As an example, LAS glass–ceramics comprising primarily of β-quartz solid solution phase can have near zero TEC, while the crystallization of lithium silicate phases can result in a TEC of the order of $10–13 \times 10^{-6}\,^{\circ}C^{-1}$ [34]. In order to optimize the thermo-physical properties of the glass–ceramics, an accurate phase characterization is thus essential. Complementary to XRD, which is the most common method for phase identification, NMR is a powerful tool for such study because it enables to characterize both amorphous and crystalline samples, to observe each nucleus separately (particularly light elements like ^{11}B, which are difficult to observe in crystals with XRD), to detect phases present in very low amount, and to quantify the proportion of crystals and amorphous phases. Moreover, the use of a high-field (18.8 T) NMR spectrometer enables to get an improved resolution for quadrupolar nuclei like ^{27}Al and ^{11}B.

According to the continuous random network theory (CRNT), Li_2O is a network modifying oxide [35]. A reduction in modifier oxide content is expected to increase the connectivity of the network, leaving fewer non-bridging oxygen atoms. A network with higher connectivity is expected to exhibit improved mechanical cohesion, thus explaining the observed increase in micro-hardness. In addition, the more rigid network is at the origin of the observed reduction in the TEC.

While the thermo-physical properties change linearly with the modifier fraction, ^{29}Si NMR indicates an abrupt change in the network polymerization on going from L2 to L3 glasses, although there is no major change from L2 to L3 glasses in terms of composition. The change in the network leading to this change in peak shape could arise as a consequence of a reduction in the number of Al or B atoms in the second coordination sphere of silicon, since the presence of these atoms moves the Q^n chemical shift to positive values [25,26]. The presence of some silica-rich phase separation may also be at the origin of the ^{29}Si shift,

although we could get no experimental evidence for this. Phase separation in lithium silicate glasses induced by phosphates was indeed reported by Holland et al. [15].

The ^{29}Si MAS-NMR spectrum of the L1 glass–ceramic shows a narrow resonance characteristic of lithium disilicate at ~ -92 ppm. Lithium disilicate phase is made up of Si in Q^3 speciation [17] and the crystallization of this phase leaves a residual glass enriched in Al and B. Thus, the crystallization of lithium disilicate shifts the Q^4 resonance of the residual glass to less negative values (-104 ppm). A similar feature is observed in L2 glass–ceramics as well.

For glass–ceramics derived from L4 and L5 samples, XRD indicates the presence of quartz and an alumino-silicate phase, virgilite $Li_xAl_xSi_{(3-x)}O_6$. No ^{29}Si chemical shift data are available for the latter phase. However, ^{27}Al NMR spectra did not showed any difference between glasses and glass–ceramics. Hence, we must consider the ^{11}B NMR spectra of the glasses and glass–ceramics.

The ^{11}B NMR spectra of LAS glasses evolve as expected with the decreasing alkali oxide fraction. Indeed, the decrease in the alkali fraction means less alkali ions are available for charge compensation of BO_4 units, which can explain the increase in BO_3 proportion with a reduction in the modifier fraction [24].

^{11}B NMR spectra of glass–ceramics show an interesting feature. Generally, B_2O_3 containing phase is not expected to devitrify from multicomponent glass compositions. However, the ^{11}B spectra shown in Fig. 8 reveal sharp peak at -3.3 ppm. The sharp peak indicates the formation of regular crystalline environments. It is likely that this phase can be connected to the -113 ppm peak observed in ^{29}Si NMR. The ^{27}Al NMR spectra of the glasses and glass–ceramics are almost identical and this shows that Al^{3+} ions are not participating in the formation of crystalline phases. Therefore, we must rule out the presence of any Al containing phase such as eucryptite or spodumene that may be expected according to the position of the composition in the LAS phase diagram. Moreover, the ^{29}Si chemical shifts of these compounds are -100 and -90.6 ppm [36], respectively, which are not compatible with the observed value at -113 ppm. This seems to call into question the phase assignment of XRD diagrams of L4 and L5 glass–ceramics, in which the alumino-silicate phase virgilite ($Li_xAl_xSi_{3-x}O_6$) was tentatively identified.

However, taking into account that no Al is present in the crystal but boron is present, we conclude that the phase detected by XRD is more likely a phase isomorphous to virgilite: lisitsynite $KBSi_2O_6$. A similar lithium containing phase, or a mixed alkali phase $(Li,K)BSi_2O_6$ is probably also present. This lisitsynite phase is structurally similar to virgilite, which in turn is similar to eucryptite. Indeed, most known crystalline borosilicates are structurally similar to aluminosilicates (leucite family, feldspars, zeolites and others) [37]. Although the crystallization of this lisitsynite phase from borosilicate glasses (without alumina) was already observed [38], to the best of our knowledge its crystallization was never reported in multicomponent alumino-borosilicate glasses. The ambiguity in XRD phase assignment is a result of XRD being unable to discern Al from B. To the best of our knowledge, there are no references for the ^{11}B or ^{29}Si chemical shifts in (Li, K)BSi_2O_6 type phases, so we assume that the -113 ppm peak in the ^{29}Si NMR spectra of LAS glass–ceramics may be assigned to $(Li,K)BSi_2O_6$ phase.

With the decrease in the alkali oxide content, the fraction of crystalline phases reduces. The present glass–ceramics were formulated with the expectation that a high Al_2O_3 content would result in the formation of stable, charge compensated corner linked AlO_4 and PO_4 tetrahedra that would impede the phase separation action of P_2O_5 [39]. This is in agreement with the DTA studies carried out previously, which indicated that crystallization becomes more difficult with a decrease in the Li_2O fraction [13]. The P_2O_5 is incorporated into the glass as a nucleating agent [40]. The Gaussian lineshape of the ^{31}P NMR spectra of the glasses indicate that the P atoms are mainly present in an amorphous environment. However, the ^{31}P NMR spectra of L3 and L5 glasses showed the formation of Li_3PO_4. This phase could not be detected from XRD, since the amount of the phase was less than the detection limit. In the glass–ceramics, at lower alumina concentrations, Li_3PO_4 is the major phosphate phase. Beyond L3, it is evident that K atoms also participate in the crystallization process. Thus the peak has an additional contribution from a K containing orthophosphate phase. If we consider the L5 glass–ceramics where the shoulder is most clearly expressed, the peak is clearly made up of two Lorentzian resonances at 9.9 and 10.3 ppm, corresponding to Li_3PO_4 and $(Li, K)_3PO_4$ phases, respectively. It is known that pure K_3PO_4 has a chemical shift of 11.7 ppm, while Li_3PO_4 is expected to show a chemical shift of 10 ppm. A chemical shift of 10.32 ppm indicates the crystallization of a $K_{3-x}Li_xPO_4$ solid solution, while the Lorentzian peak shape is an indicator of a regular crystalline environment. This can be compared to the disordered environment in the $Na_{3-x}Li_xPO_4$ solid solution that we observed in other lithium–sodium zinc silicate glass–ceramics [21].

In the glasses beyond L3 (i.e. having higher alumina content), it is likely that the $K_{3-x}Li_xPO_4$ precipitates when not enough Li^+ are available for the charge compensation of Li_3PO_4, since they are also involved in the charge compensation of several silicate crystalline phases.

5. Conclusion

The use of MAS-NMR enables an accurate characterization of the amorphous and crystalline phases, complementary to XRD. While quartz detection is not easy with NMR, ^{29}Si NMR in conjunction with ^{11}B NMR allowed the identification of a boron containing silicate phase, $(Li,K)BSi_2O_6$, that could not be distinguished from the aluminosilicate virgilite $Li_xAl_xSi_{(3-x)}O_6$ with XRD. This was confirmed by the ^{27}Al NMR spectra that ruled out the presence of any Al containing phase. Further investigations are under way in order to quantify the proportion of the amorphous and crystalline phases in the samples, and to characterize the specific effect of the $(Li,K)BSi_2O_6$ phase on the glass–ceramics properties

The ^{31}P NMR spectra of the LAS glass–ceramics indicate the crystallization of two types of orthophosphates: Li_3PO_4 and $(Li,K)_3PO_4$, which could not be detected with XRD and probably act as nucleating agent. The amount of the mixed Li,K orthophosphate phase increases with Al_2O_3 concentration since not enough Li^+ ion is available for the charge compensation of PO_4 groups.

Acknowledgments

The authors will like to thank Drs. V.C. Sahni and J.V. Yakhmi for encouragement and support. They would like to thank Mr. V.K. Shrikhande and Dr. Madhumita Goswami for technical discussion and to Mr. Arjun Sarkar for help in preparation of samples. The FEDER, Region Nord Pas-de-Calais, Ministère de l'Education Nationale de l'Enseignement Superieur et de la Recherche, CNRS, and USTL are acknowledged for funding of NMR spectrometers. One of the authors (AA) thanks the DAE for awarding him a fellowship.

Appendix A. Supplementary material

Supplementary data associated with this article can be found in the online version at doi:10.1016/j.jssc.2009.10.006.

References

[1] H. Zhaoxia, S. Chunhui, Z. Yongming, Z. Huashan, Z. Hongbo, S. Jing, M. Qingxin, J. Rare Earths 24 (2006) 418–422.
[2] M. Chatterjee, M.K. Naskar, Ceram. Int. 32 (2006) 623–632.
[3] K. Cheng, Mater. Sci. Eng. B 60 (1999) 194–199.
[4] P.F. James, J. Non-Cryst. Solids 181 (1995) 1–15.
[5] P. Riello, P. Canton, N. Comelato, S. Polizi, M. Verità, G. Fagherazzi, H. Hofmeister, S. Hopfe, J. Non-Cryst. Solids 288 (2001) 127–139.
[6] Y.M. Sung, S.A. Dunn, J.A. Koutsky, J. Eur. Ceram. Soc. 14 (1994) 455–462.
[7] H. Scheidler, J. Thürk, The ceran-top-system®: high tech appliance for the kitchen, in: H. Bach (Ed.), Low Thermal Expansion Glass–Ceramics, Springer, Berlin, 1995, pp. 51–60.
[8] M. Bengisu, R.K. Brow, J. Non-Cryst. Solids 331 (1–3) (2003) 137–144.
[9] A. Ananthanarayanan, R. Kumar, S. Bhattacharya, V.K. Shrikhande, G.P. Kothiyal, J. Phys. Conf. Ser. 114 (2008) 012042–012048.
[10] I.W. Donald, J. Mater. Sci. 28 (11) (1993) 2841–2886.
[11] M. Albakry, M. Guazzato, M.V. Swain, J. Prosthet. Dent. 13 (3) (2004) 141–149.
[12] M. Dündar, M. Özcan, B. Gökçe, E. Çömlekoğlu, F. Leite, L.F. Valandro, Dent. Mater. 23 (5) (2007) 630–636.
[13] A. Ananthanarayanan, A.K. Tyagi, R. Mishra, V.K. Shrikhande, G.P. Kothiyal, Phys. Chem. Glasses Eur. J. Glass Sci. Technol. B 49 (3) (2008) 166–173.
[14] C. Siligardi, L. Barbieri, A. Bonamartini Corradi, C. Leonelli, M. De Sanctis, A. Lazzeri, Phys. Chem. Glasses 41 (2) (2000) 81–88.
[15] D. Holland, Y. Iqbal, P. James, B. Lee, J. Non-Cryst. Solids 232–234 (1998) 140–146.
[16] R. Dupree, D. Holland, M.G. Mortuza, J. Non-Cryst. Solids 116 (1990) 148–160.
[17] C.M. Schramm, B.H.W.S. De Jong, V.E. Parziale, J. Am. Ceram. Soc. 106 (16) (1984) 4396–4402.
[18] N.J. Clayden, N. Esposito, U.A. Jayasooriya, J. Sprunt, P. Pernice, J. Non-Cryst. Solids 224 (1998) 50–56.
[19] L. Olivier, X. Yuan, A.N. Cormack, C. Jäger, J. Non-Cryst. Solids 293–295 (2001) 53–66.
[20] D. Massiot, F. Fayon, M. Capron, I. King, S. Le Calve, B. Alonso, J.O. Durand, B. Bujoli, Z. Gan, G. Hoatson, Magn. Reson. Chem. 40 (2002) 70–76.
[21] M. Goswami, G.P. Kothiyal, L. Montagne, L. Delevoye, J. Solid State Chem. 181 (2008) 269–275.
[22] J. Ramkumar, V. Sudarsan, S. Chandramouleeswaran, V.K. Shrikhande, G.P. Kothiyal, P.V. Ravindran, S.K. Kulsreshta, T. Mukherjee, J. Non-Cryst. Solids 354 (2008) 1591–1597.
[23] A. Hamoudi, L. Kouchaf, C. Depecker, B. Revel, L. Montagne, P. Cordier, J. Non-Cryst. Solids 354 (2008) 5074–5078.
[24] H. Maekawa, T. Maekawa, K. Kawamura, T. Yokokawa, J. Non-Cryst. Solids 127 (1991) 53–64.
[25] A. Stamboulis, R.G. Hill, R.V. Law, J. Non-Cryst. Solids 333 (2004) 101–107.
[26] B.G. Parkinson, D. Holland, M.E. Smith, A.P. Howes, C.R. Scales, J. Non-Cryst. Solids 351 (2005) 2425–2432.
[27] K.J.D. MacKenzie, M.E. Smith, Multinuclear Solid State NMR of Inorganic Materials, Pergamon Press, 2002 p. 212.
[28] G. Engelhardt, R. Radeglia, J. Chem. Phys. Lett. 108 (3) (1984) 271–274.
[29] J.F. Stebbins, S. Kroecker, S.K. Lee, T.J. Kiczenski, J. Non-Cryst. Solids 275 (1–6) (2000) 2425–2432.
[30] G.D. Cody, B. Mysen, G. Sághi-Szabó, J.A. Tossell, Geochim. Cosmochim. Acta 65 (14) (2001) 2395–2411.
[31] A.R. Grimer, U. Haubenreisser, Chem. Phys. Lett. 99 (1983) 487–490.
[32] K.J.D. MacKenzie, M.E. Smith, Multinuclear Solid State NMR of Inorganic Materials, Pergamon Ed. 2002, p. 439.
[33] L.-S. Du, J.F. Stebbins, J. Non-Cryst. Solids 315 (2003) 239–255.
[34] P.W. Macmillan, Glass–Ceramics, Academic Press, New York, 1977 p. 176.
[35] J.E. Shelby, R. Soc. Chem. (RSC) (1997) 86–89.
[36] A. Nordmann, Y.B. Cheng, T.J. Bastow, A.J. Hill, J. Phys. Condens. Matter 7 (1995) 3115–3128.
[37] M.G. Krzhizhanovskaya, R.S. Bubnova, S.K. Filatov, Minerals as Advanced Materials (I), Springer, Berlin, Heidelberg, 2008, pp. 117–121.
[38] M.I. Georgievskaya, R.S. Bubnova, S.K. Filatov, Glass Phys. Chem. 34 (4) (2008) 430–442.
[39] J.Y. Hsu, R.F. Speyer, J. Am. Ceram. Soc. 72 (12) (1989) 2334–2341.
[40] T.J. Headley, R.J. Loehman, J. Am. Ceram. Soc. 67 (9) (1984) 354–361.